# Microwave Frequency Measurement Based on an Optically Injected Semiconductor Laser

Bowen Zhang, Dan Zhu, *Member, IEEE*, Hao Chen, Yuewen Zhou, and Shilong Pan, *Senior Member, IEEE*

***Abstract*— A microwave frequency measurement system utilizing the optical injection technology in a semiconductor laser is proposed. A single-wavelength optical carrier is generated and divided into two parts. One part is intensity-modulated by a control signal with a triangular shape and then injected into a semiconductor laser to generate a frequency scanning optical sideband. The other part is modulated by the microwave signal under test, which is then coupled with the frequency scanning optical sideband and detected by a photodetector (PD). The output of the PD is filtered by an electrical passband filter and detected by an envelope detector. Electrical pulses will be obtained with the time interval proportional to the microwave frequency. Thus the microwave frequency can be retrieved from the time interval of the generated pulses. A proof of concept experiment is taken. The microwave frequency measurement from 3 to 40 GHz is achieved, and the frequency measurement errors are within ±30 MHz.**

***Index Terms*— Microwave frequency measurement, optical injection, semiconductor laser.**

## I. Introduction

MICROWAVE frequency measurement plays an important role in many applications, e.g., electronic warfare, radar, wireless communication systems [1]–[3]. Conventionally, microwave frequency can be identified by electrical methods [4], but the measurement speed and bandwidth are usually limited. To solve these problems, photonic approaches mapping the microwave frequency into time domain have been proposed for the microwave frequency measurement [5]–[15]. One typical method is based on the time-division multiplexing (TDM) technique, which is usually performed using a frequency-shifted loop [5]–[7]. After electro-optical modulation and several rounds in the loop, the optical carrier and the frequency-shifted sideband are combined and photodetected, generating a down-converted microwave signal. Utilizing the temporal position of the generated signal, the microwave frequency can be obtained. However, the operation time will increase with the measured bandwidth.

To realize a fast frequency measurement, real-time Fourier transformation (RTFT) is proposed [8]–[11], which can be implemented using a dispersion element assisted with a time lens [9], [10]. However, the frequency resolution is usually limited by the dispersion value. Although an improved resolution can be realized using a frequency-shifted feedback laser [11], it is hard to simultaneously achieve a large instantaneous bandwidth and a high frequency resolution.

Another typical method is the photonics-based frequency scanning measurement [12]–[15]. A narrow-band filter, of which the passband position is varying with time, is utilized to filter the optical-carried microwave signal. A temporally varying optical power after the filter is generated, which is the mapping of the microwave spectrum. The narrow-band filter can be implemented using a microwave photonic filter assisted by a linear frequency modulated signal (LFM) generator [14], [15]. A high-speed digital-analog converter is required in [14] and the continuous measurement of the microwave frequency is hard to realize in [15].

In this letter, utilizing the optical injection technology in a semiconductor laser, a microwave frequency measurement scheme is proposed. A single-wavelength optical carrier emitted from a master laser (ML) is divided into two parts. One part is intensity-modulated by a control signal with a triangular shape. By injecting the intensity-modulated optical carrier into a semiconductor slave laser (SL) working at the period-one state, a frequency scanning optical sideband is generated. The other part of the optical carrier is modulated by the microwave signal under test, generating the optical signal sideband. The optical signal sideband and the frequency scanning optical sideband are coupled together and detected by a PD. Then the electrical passband filtering and the envelope detection are carried out, generating the electrical pulses. The frequency of the signal under test will be retrieved from the time interval of the generated pulses. As compared with [14], only a digital-analog converter with a sampling rate as low as 2 GSa/s is required. In the experimental demonstration, a frequency measurement region of 3-40 GHz and frequency errors of ±30 MHz are realized. The frequency resolution as low as 11 MHz can be realized with the help of a 20-MSa/s oscilloscope.

## II. Principle and Experimental Results

Fig. 1 shows the scheme of our proposed system. An optical carrier with a frequency of $f_0$ is emitted from the ML and divided into two parts. Via a Mach-Zehnder modulator (MZM1), the microwave signal under test, of which the frequency is assumed to be $f_m$, modulates one part of the optical carrier. The first-order sideband is selected by an optical bandpass filter (OBPF1), which performs the optical signal sideband and can be mathematically expressed as

$$E_{up}(t) = E_1 \exp\left[j2\pi\left(f_0 + f_m\right)t\right] \tag{1}$$

where $E_1$ represents the optical signal amplitude after OBPF1. The direct digital synthesizer (DDS) generates a control signal

Manuscript received September 10, 2020; revised October 17, 2020; accepted October 26, 2020. Date of publication November 3, 2020; date of current version November 17, 2020. This work was supported in part by the National Natural Science Foundation of China under Grant 61971222 and in part by the Fundamental Research Funds for Central Universities under Grant NE2017002 and Grant NC2018005. *(Corresponding authors: Dan Zhu; Shilong Pan.)*

The authors are with the College of Electronic and Information Engineering, Nanjing University of Aeronautics and Astronautics, Nanjing 210016, China (e-mail: danzhu@nuaa.edu.cn; pans@nuaa.edu.cn).

Color versions of one or more figures in this article are available at https://doi.org/10.1109/LPT.2020.3035694.

Digital Object Identifier 10.1109/LPT.2020.3035694

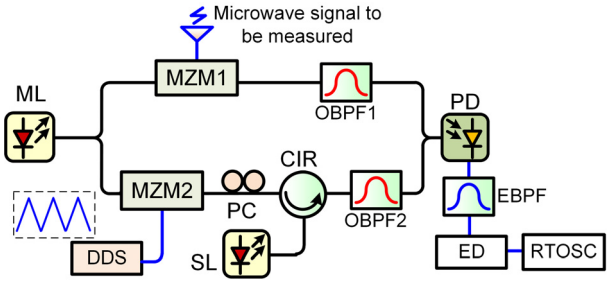


Fig. 1. Schematic configuration of the proposed system. ML, master laser; MZM, Mach–Zehnder modulator; OBPF, optical bandpass filter; PC, polarization controller; CIR, circulator; DDS, direct digital synthesizer; SL, slave laser; PD, photodetector; EBPF, electrical bandpass filter; ED, envelope detector; RTOSC, real-time oscilloscope.

with a triangular shape, which is used to intensity-modulate the other part of the optical carrier via MZM2. A polarization controller (PC) is used to realize an optimal injection efficiency of the SL, which works at the period-one state. The output of the SL is filtered by OBPF2 to remove the optical carrier. The frequency scanning optical sideband will be generated, which can be mathematically expressed as

$$E_{down}(t) = \begin{cases} E_2 \exp\left\{ j2\pi \left[ \left( f_0 + f_c + \frac{1}{2} f_{\mathrm{BW}} \right) t + \frac{f_{\mathrm{BW}}}{T_{\mathrm{tri}}} t^2 \right] \right\} \\ \qquad when \quad -\frac{T_{\mathrm{tri}}}{2} \le t \le 0 \\ E_2 \exp\left\{ j2\pi \left[ \left( f_0 + f_c + \frac{1}{2} f_{\mathrm{BW}} \right) t - \frac{f_{\mathrm{BW}}}{T_{\mathrm{tri}}} t^2 \right] \right\} \\ \qquad when \quad 0 \le t \le +\frac{T_{\mathrm{tri}}}{2} \end{cases} \tag{2}$$

where $E_2$ is the amplitude of the optical signal, $f_0 + f_c$, $f_{\mathrm{BW}}$, and $T_{\mathrm{tri}}$ are the central frequency, spectrum width, and period of the frequency scanning optical sideband, respectively. It is worthy to note that $f_0 + f_c$, $f_{\mathrm{BW}}$, and $T_{\mathrm{tri}}$ are related to the power of the injected optical signals, the half-wave voltage ($V_\pi$) of MZM2, and the waveform of the applied control signal [16].

The output of the two branches are combined and injected into a PD, with the electrical output as (3), shown at the bottom of the page.

As can be seen, a triangular LFM signal with the instantaneous frequency of $f_c$+0.5$f_{\mathrm{BW}}$-$f_m$+2$f_{\mathrm{BW}}t/T_{\mathrm{tri}}$ during -$T_{\mathrm{tri}} \le t \le$0 and $f_c$+0.5$f_{\mathrm{BW}}$-$f_m$-2$f_{\mathrm{BW}}t/T_{\mathrm{tri}}$ during $0 \le t \le T_{\mathrm{tri}}$ is generated. After passing through an electrical bandpass filter (EBPF, center frequency $f_{\mathrm{IF}}$, bandwidth $\delta f_{\mathrm{IF}}$) and an envelope detector, the output signal can be expressed as

$$E_{out}(t) = \delta\left[ t - \frac{f_m + f_{IF} - (f_c + 0.5 f_{\mathrm{BW}})}{2 f_{\mathrm{BW}}} T_{\mathrm{tri}} \right] + \delta\left[ t + \frac{f_m + f_{IF} - (f_c + 0.5 f_{\mathrm{BW}})}{2 f_{\mathrm{BW}}} T_{\mathrm{tri}} \right] \tag{4}$$

where $\delta(t)$ represents the temporal envelope of the generated pulse and is related to the frequency response of EBPF. The two pulses have a microwave frequency-dependent time interval, which can be expressed as

$$\Delta\tau = \frac{(f_c + 0.5 f_{\mathrm{BW}}) - (f_m + f_{IF})}{f_{\mathrm{BW}}} T_{\mathrm{tri}} \tag{5}$$

Thus the microwave frequency under test is mapped into time domain with a mapping factor of $T_{\mathrm{tri}}/f_{\mathrm{BW}}$. By analyzing the temporal output signal, the microwave frequency can be estimated.

## III. Experimental Results and Discussion

Based on the analysis above, an experiment is conducted. A tunable laser diode (Agilent N7714A) is used as the ML. MZM1 (Fujitsu FTM7938EZ, 40-GHz bandwidth, 4-V $V_\pi$) is driven by the signal under test from a microwave signal generator (Agilent E8267D, 250 kHz-67 GHz) and MZM2 (Lucent 2623NA, 10-GHz bandwidth, 3.5-V $V_\pi$) is driven by a control signal with a triangular shape from a 2-GSa/s DDS (Agilent 81150A). A distributed feedback semiconductor laser (Actech LD15DM) is used as the SL. The bandwidth of the PD is 30 GHz. The central frequency and the bandwidth of the EBPF are 10 GHz and 11 MHz, respectively. Two OBPFs (Yenista XTM-50, out-of-band suppression ratio larger than 40 dB) are used to remove the optical carriers in the upper and lower branches. The envelope detector (ED, Agilent 8474C) has a working frequency range of 10 MHz-33 GHz. The real-time oscilloscope (RTOSC, Keysight DSO-X 92504A) has a tunable sampling rate up to 80 GSa/s.

Firstly, an optical carrier with a wavelength of 1543.839 nm and a power of 16 dBm is emitted from the ML. After passing through MZM2, the PC and the circulator, the optical power injected into the SL is about 6 dBm. The wavelength of the free-running SL is 1543.932 nm, thus the frequency detuning is 0.093 nm. When MZM2 is not driven by any signal, the spectrum of the signal after the PC is measured by an optical spectrum analyzer (APEX AP2040D, resolution 0.04 pm) and plotted in Fig. 2(a). Meanwhile, the optical spectra of the SL without and with injection are also plotted in Fig. 2(a). The frequency spacing of the longitudinal modes shown as the blue curve in Fig. 2(a) is about 0.18 nm (corresponding to the period-one frequency). When MZM2 is driven by a control

$$E_{PD}(t) = \eta_{PD} \left| E_{up}(t) + E_{down}(t) \right|^2 = \begin{cases} \eta_{PD} \left( E_1^2 + E_2^2 + 2E_1E_2 \cos 2\pi \left[ \left( f_c + \frac{1}{2} f_{\mathrm{BW}} - f_m \right) t + \frac{f_{\mathrm{BW}}}{T_{\mathrm{tri}}} t^2 \right] \right) \\ \qquad when \quad -\frac{T_{\mathrm{tri}}}{2} \le t \le 0 \\ \eta_{PD} \left( E_1^2 + E_2^2 + 2E_1E_2 \cos 2\pi \left[ \left( f_c + \frac{1}{2} f_{\mathrm{BW}} - f_m \right) t - \frac{f_{\mathrm{BW}}}{T_{\mathrm{tri}}} t^2 \right] \right) \\ \qquad when \quad 0 \le t \le +\frac{T_{\mathrm{tri}}}{2} \end{cases} \tag{3}$$

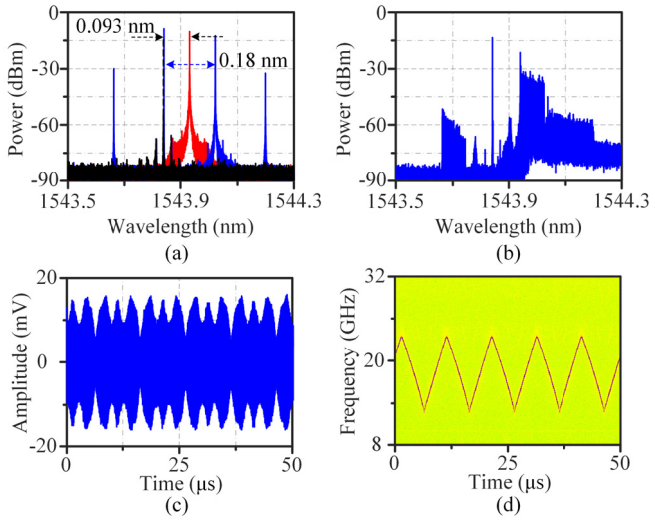


Fig. 2. (a) Optical spectra of the injecting light (black dashed curve), the SL without injection (red curve), and the SL with injection (blue curve). (b) The optical spectrum of the SL with injection when a control signal is applied, and (c) the waveform, (d) time-frequency diagram of the correspondingly generated electrical signal.

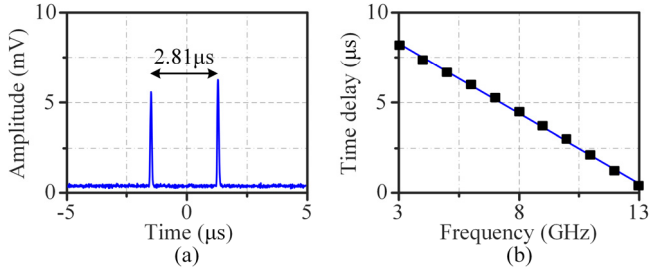


Fig. 3. (a) The experimental measurement result of a 10-GHz signal. (b) The measured time interval value of the two generated pulses versus the microwave frequency value tuning from 3 to 13 GHz.

signal with a triangular shape, of which the voltage varies from -1.8 V to 0.7 V and the period is 10 $\mu$s, the optical spectrum of the SL with injection is shown in Fig. 2(b). To observe the frequency scanning optical sideband, the optical signal before the OBPF2 is sent to the PD. The generated signal is captured by the RTOSC and plotted in Fig. 2(c). The process of time-frequency analysis for the generated signal is carried out to obtain the instantaneous frequency, which is shown in Fig. 2(d). A frequency scanning optical sideband with a spectrum width of 11 GHz (12.1-23.1 GHz) and a period of 10 $\mu$s is generated.

Then a 10-GHz signal with a 10-dBm power is used to drive MZM1. By setting the sampling rate of the RTOSC to be 100 MSa/s, the output waveform of the system is recorded and plotted in Fig. 3(a). A 2.81-$\mu$s time interval of the two generated pulses is observed, which is consistent with (5). The measurement region of the microwave frequency is from $f_c$-0.5$f_{\mathrm{BW}}$ + $f_{\mathrm{IF}}$ to $f_c$+0.5$f_{\mathrm{BW}}$ + $f_{\mathrm{IF}}$, which is 2.1-13.1 GHz in this experiment. By adjusting the microwave frequency from 3 to 13 GHz with a spacing of 1 GHz, different time interval values of the two pulses are measured and shown in Fig. 3(b).

It is worthy to note that (4) is obtained on the condition that $f_c$+0.5$f_{\mathrm{BW}}$-$f_m$±2$f_{\mathrm{BW}}t/T_{\mathrm{tri}}$ = $f_{\mathrm{IF}}$. In fact, due to the square-law detection of the PD, when $f_c$+0.5$f_{\mathrm{BW}}$-$f_m$±2$f_{\mathrm{BW}}t/T_{\mathrm{tri}}$ = $-f_{\mathrm{IF}}$, two pulses can also be observed in

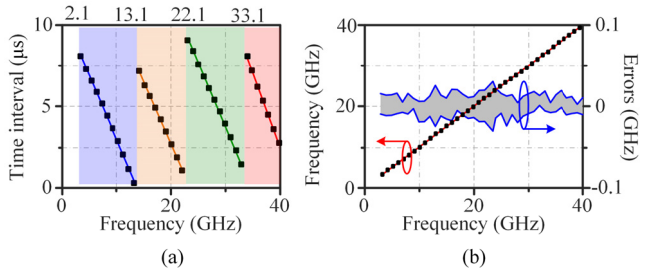


Fig. 4. (a) The measured pulse interval value versus the microwave frequency. (b) The retrieved frequency and measurement errors of 100 times. The solid lines: theoretical results, solid dots: measured results.

the RTOSC. Thus the frequency component from $f_c$-0.5$f_{\mathrm{BW}}$-$f_{\mathrm{IF}}$ to $f_c$+0.5$f_{\mathrm{BW}}$-$f_{\mathrm{IF}}$ can also be measured, which is from 22.1 to 33.1 GHz in this experiment. Meanwhile, it has been experimentally demonstrated that the frequency spacing between the optical carrier and the frequency scanning optical sideband is adjustable by changing the optical power and wavelength of the ML, and the waveform of the applied control signal [16]. Thus the measurement region of this system is adjustable. In detail, by adjusting the injection parameters, the spectrum of the generated electrical signal in Fig. 2(d) will be from 23.1 to 32.1 GHz. Thus the frequency measurement ranges will be 13.1-22.1 GHz and 33.1-42.1 GHz, corresponding to the second and the fourth sliced regions in Fig. 4(a). In this experiment, microwave frequency measurements in the region of 3-40 GHz with a spacing of 1 GHz have been carried out. Fig. 4(a) shows the measurement results in different frequency measurement intervals. Utilizing the results in Fig. 4(a), retrieved microwave frequencies are obtained, shown in Fig. 4(b).

By observing the output signals 100 times, the measurement errors are obtained and also shown in Fig. 4(b). The measurement errors in the region of 3-40 GHz are about ±30 MHz, which is mainly due to the wavelength drift of the SL and can be reduced by introducing accurate temperature and bias current controls of the SL. In addition, by using a frequency-sweeping OEO which contains optical injection and optical-electrical feedback [17], the measurement errors introduced by the SL can be further reduced.

The frequency measurement resolution in this system depends on the product between the chirp rate of the frequency scanning optical sideband ($2f_{\mathrm{BW}}/T_{\mathrm{tri}}$) and the pulse width ($\delta\tau$) of the output electrical signal. $\delta\tau$ can be mathematically expressed as

$$\delta\tau = \max\left(\frac{0.7}{\delta f_{IF}}, \frac{\delta f_{IF}}{f_{BW}} \times \frac{T_{\mathrm{tri}}}{2}\right) \tag{6}$$

where $0.7/\delta f_{\mathrm{IF}}$ represents the time width of the narrowest pulse that can be observed by the RTOSC [14]. The value of $\delta f_{\mathrm{IF}} T_{\mathrm{tri}}/2f_{BW}$ is the time duration of the filtered signal with the frequency varying from $f_{\mathrm{IF}}$-0.5$\delta f_{\mathrm{IF}}$ to $f_{\mathrm{IF}}$+0.5$\delta f_{\mathrm{IF}}$. Then the frequency measurement resolution can be calculated as follows

$$\begin{aligned}\delta f_{RBW} &= \delta\tau \cdot \left(2f_{BW}/T_{\mathrm{tri}}\right) \\ &= \max\left(\frac{1.4f_{BW}}{\delta f_{IF} T_{\mathrm{tri}}}, \delta f_{IF}\right)\end{aligned} \tag{7}$$

It can be inferred from (7) that the optimal frequency resolution can be achieved with the value of $\delta f_{\mathrm{IF}}$ on the condition

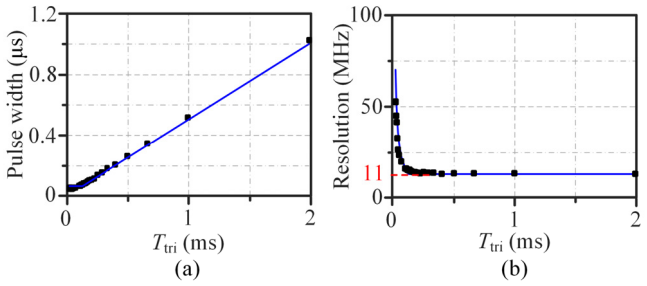


Fig. 5. (a) Pulse width ($\delta\tau$) of the output electrical signal and (b) the theoretical frequency resolution versus the time duration $T_{\text{tri}}$ of the control signal. Solid dots: experimental results, blue curve: simulated theoretical results.

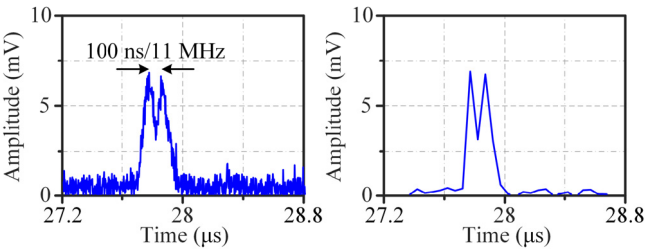


Fig. 6. System outputs of a two-tone signal with a frequency difference of 11 MHz (10 and 10.011 GHz). (a) Sampling rate 100 MSa/s. (b) Sampling rate 20 MSa/s.

that $T_{\text{tri}} > 1.4 f_{BW}/\delta f_{\text{IF}}^2$. To demonstrate this, in the experiment, $f_{\text{BW}}$ and $\delta f_{\text{IF}}$ are set to be 11 GHz and 11 MHz, respectively. Fig. 5(a) shows the experimentally obtained pulse width values ($\delta\tau$) of the output electrical signals by tuning $T_{\text{tri}}$ of the applied control signal, as shown in solid dots. The corresponding frequency resolution values are also calculated according to (7), as shown in solid dots in Fig. 5(b). Meanwhile, the theoretical results are also calculated according to (6) and (7), as shown in Fig. 5(a) and Fig. 5(b) in blue curves. As can be seen, the experimental results agree well with the theoretical analyses. In addition, from Fig. 5 (b), it can be seen that with the increasing of the $T_{\text{tri}}$ value, the system resolution is limited to about 11 MHz (the bandwidth $\delta f_{\text{IF}}$ of the EBPF), which also agrees well with the theoretical analyses.

To further verify this, an experiment is carried out with $T_{\text{tri}}$ being set as 200 $\mu$s. A two-tone signal with a frequency difference of 11 MHz (10 and 10.011 GHz) is used to drive MZM1. Fig. 6 (a) shows the system output. It can be seen that the mapping results from this two-tone signals can be identified, approving the frequency resolution of no more than 11 MHz. The frequency resolution of this system can be further improved utilizing an EBPF with a smaller bandwidth, simultaneously along with a larger period of the control signal. Besides, to observe the system output, the maximum sampling interval must be less than $0.5\delta\tau$, which is 50 ns in this experiment. Therefore, the sampling rate of the RTOSC can be as low as 20 MSa/s. On this condition, when the same two-tone microwave signal is applied, the system output is recorded and plotted in Fig. 6 (b), which shows a great consistence with Fig. 6 (a). This required sampling rate of the RTOSC can be reduced using an electrical triangular control signal with a larger time duration.

## IV. Conclusion

In this letter, we propose and experimentally demonstrate a microwave frequency measurement scheme utilizing the optical injection technology in a semiconductor laser. Microwave frequency measurement form 3 to 40 GHz is realized. Measurement errors are within ±30 MHz. A frequency resolution no larger than 11 MHz has been realized using an RTOSC with a sampling rate as low as 20 MSa/s. This scheme provides a possible solution to modern spectrum measurement system.

## References

[1] C.-H. Cheng, D. M. Lin, L. L. Liou, and J. B. Tsui, "Electronic warfare receiver with multiple FFT frame sizes," *IEEE Trans. Aerosp. Electron. Syst.*, vol. 48, no. 4, pp. 3318–3330, Oct. 2012.

[2] D. Zhu and S. Pan, "Broadband cognitive radio enabled by photonics," *J. Lightw. Technol.*, vol. 38, no. 12, pp. 3076–3088, Jun. 15, 2020.

[3] M. Agiwal, A. Roy, and N. Saxena, "Next generation 5G wireless networks: A comprehensive survey," *IEEE Commun. Surveys Tuts.*, vol. 18, no. 3, pp. 1617–1655, 3rd Quart., 2016.

[4] A. O. Benz *et al.*, "A broadband FFT spectrometer for radio and millimeter astronomy," *Astron. Astrophys.*, vol. 442, no. 2, pp. 767–773, Nov. 2005.

[5] T. A. Nguyen, E. H. W. Chan, and R. A. Minasian, "Photonic radio frequency memory using frequency shifting recirculating delay line structure," *J. Lightw. Technol.*, vol. 32, no. 1, pp. 99–106, Jan. 1, 2014.

[6] T. A. Nguyen, E. H. W. Chan, and R. A. Minasian, "Photonic multiple frequency measurement using a frequency shifting recirculating delay line structure," *J. Lightw. Technol.*, vol. 32, no. 20, pp. 3831–3838, Oct. 15, 2014.

[7] H. Chen *et al.*, "Photonics-assisted serial channelized radio-frequency measurement system with Nyquist-bandwidth detection," *IEEE Photon. J.*, vol. 6, no. 6, pp. 1–7, Dec. 2014.

[8] B. Zhang *et al.*, "Impact of dispersion effects on temporal-convolution-based real-time Fourier transformation systems," *J. Lightw. Technol.*, vol. 38, no. 17, pp. 4664–4676, Sep. 1, 2020.

[9] R. Salem, M. A. Foster, and A. L. Gaeta, "Application of space-time duality to ultrahigh-speed optical signal processing," *Adv. Opt. Photon.*, vol. 5, pp. 274–317, Aug. 2013.

[10] C. Wang, "Dispersive Fourier transformation for versatile microwave photonics applications," *Photonics*, vol. 1, no. 4, pp. 586–612, Dec. 2014.

[11] H. G. de Chatellus, L. R. Ortés, and J. Azaña, "Optical real-time Fourier transformation with kilohertz resolutions," *Optica*, vol. 3, no. 1, pp. 1–8, 2016.

[12] P. Ghelfi, F. Scotti, D. Onori, and A. Bogoni, "Photonics for ultrawideband RF spectral analysis in electronic warfare applications," *IEEE J. Sel. Topics Quantum Electron.*, vol. 25, no. 4, pp. 1–9, Jul. 2019.

[13] S. Song *et al.*, "Photonic-assisted scanning receivers for microwave frequency measurement," *Appl. Sci.*, vol. 9, no. 2, p. 328, Jan. 2019.

[14] J. Shi, F. Zhang, D. Ben, and S. Pan, "Simultaneous radar detection and frequency measurement by broadband microwave photonic processing," *J. Lightw. Technol.*, vol. 38, no. 8, pp. 2171–2179, Apr. 15, 2020.

[15] T. F. Hao, J. Tang, N. N. Shi, W. Li, N. H. Zhu, and M. Li, "Multiple-frequency measurement based on a Fourier domain mode-locked optoelectronic oscillator operating around oscillation threshold," *Opt. Lett.*, vol. 44, no. 12, pp. 3062–3065, Jun. 2019.

[16] B. W. Zhang, D. Zhu, P. Zhou, C. X. Xie, and S. L. Pan, "Tunable triangular frequency modulated microwave waveform generation with improved linearity using an optically injected semiconductor laser," *Appl. Opt.*, vol. 58, no. 20, pp. 5479–5485, Jul. 2019.

[17] P. Zhou, F. Zhang, and S. Pan, "Generation of linear frequency-modulated waveforms by a frequency-sweeping optoelectronic oscillator," *J. Lightw. Technol.*, vol. 36, no. 18, pp. 3927–3934, Sep. 15, 2018.